

Model-Based Machine Learning for Max-Min Fairness Beamforming Design in JCAS Systems

Mengyuan Ma*, Tianyu Fang*, Nir Shlezinger†, A. L. Swindlehurst§, Markku Juntti*, and Nhan Nguyen*

*Centre for Wireless Communications (CWC), University of Oulu, Finland

†School of ECE, Ben-Gurion University of the Negev, Beer-Sheva, Israel

§Department of EECS, University of California, Irvine, CA, USA

Email: {mengyuan.ma, tianyu.fang, markku.juntti, nhan.nguyen}@oulu.fi; nirshl@bgu.ac.il; swindle@uci.edu

Abstract—Joint communications and sensing (JCAS) is expected to be a crucial technology for future wireless systems. This paper investigates beamforming design for a multi-user multi-target JCAS system to ensure fairness and balance between communications and sensing performance. We jointly optimize the transmit and receive beamformers to maximize the weighted sum of the minimum communications rate and sensing mutual information. The formulated problem is highly challenging due to its non-smooth and non-convex nature. To overcome the challenges, we reformulate the problem into an equivalent but more tractable form. We first solve this problem by alternating optimization (AO) and then propose a machine learning algorithm based on the AO approach. Numerical results show that our scheme scales effectively with the number of the communications users and provides better performance with shorter run time compared to conventional optimization approaches.

Index Terms—Max-min fairness, beamforming, joint communications and sensing, machine learning.

I. INTRODUCTION

Joint communications and sensing (JCAS) is a pivotal technology for future wireless communications systems, enabling communications and sensing functionalities on a unified hardware platform. This integration facilitates spectrum sharing and reduces hardware costs [1]–[3]. However, the shared and limited resources for these dual functionalities pose significant challenges for JCAS transceiver design [4], [5]. Beamforming plays a key role in addressing this challenge by enhancing spectral efficiency and improving sensing accuracy [6], [7].

Recent literature on beamforming design for JCAS systems has focused on three main optimization goals: maximizing sensing performance, maximizing communications performance, and balancing the tradeoff between them. Sensing-oriented designs [8]–[22] optimize sensing while ensuring communication capabilities. In contrast, communication-oriented designs [23]–[25] prioritize communications performance under sensing constraints. Other works [26]–[35] explore the communications-sensing performance tradeoff by maximizing a weighted sum of communications and sensing utility functions. Communications performance is typically measured by rate or SINR, while sensing performance is evaluated using metrics like beampattern matching [8], [11]–[13], SCNR [24], [29], [31], sensing mutual information (MI) [22], [35], and the Cramér–Rao lower bound [15]–[17].

Despite these advances, achieving fairness among multiple communications users and sensing targets remains a significant challenge due to the inherently non-smooth nature of max-min

optimization problems [30]–[32]. Conventional optimization-based approaches [30]–[32] typically result in high complexity and involve numerous algorithm parameters that need to be well tuned to ensure performance. In contrast, model-based machine learning (ML) methodologies [36] facilitate real-time operation and satisfactory performance for beamforming design [5], [37]. For example, beamforming optimizers have been unfolded into deep learning models in [18]–[20], [28], [33], achieving improved computational efficiency and performance. However, current unfolded algorithms are not applicable for addressing the fairness problem because of their problem-specific network structures. Furthermore, the current literature lacks unfolded learning models specifically designed for max-min fairness problems, which typically involve complex objective functions.

In this paper, we fill this gap by jointly optimizing beamformers for both transmission and sensing, aiming to maximize the weighted sum of the minimum communications rate and sensing MI under per-antenna transmit power constraints. Given the non-smooth and non-convex nature of the problem, we first reformulate it into an equivalent but more tractable form and solve it using an alternating optimization (AO) procedure. Then, we propose a low-complexity yet efficient model-based ML method based on the AO framework. The proposed scheme retains the interpretability of conventional optimizers while achieving significantly better performance and shorter execution times. Furthermore, it scales effectively with the number of communication users, enabling seamless generalization to larger systems.

II. SYSTEM MODEL AND PROBLEM FORMULATION

JCAS System: We consider a downlink monostatic JCAS system, where a base station (BS) is equipped with N_t transmit antennas and N_r radar receive antennas. The same waveform is used for transmission and sensing [26], [29], [32]. The BS simultaneously transmits signals to K single-antenna users for communications while probing M targets. Letting $\mathbf{s} = [s_1, \dots, s_K]^T \sim \mathcal{CN}(\mathbf{0}, \mathbf{I})$ be the vector of communications symbols, and $\mathbf{W} = [\mathbf{w}_1, \dots, \mathbf{w}_K] \in \mathbb{C}^{N_t \times K}$ be the precoding matrix, the transmitted signal is expressed as $\mathbf{x} = \mathbf{W}\mathbf{s}$. We assume an equal power allocation for all antennas, such that $\text{diag}(\mathbf{W}\mathbf{W}^H) \preceq \frac{P_t}{N_t} \mathbf{1}_{N_t}$, where P_t is the transmit power budget.

The signal received by communications user k is given by

$$y_k = \mathbf{h}_k^H \mathbf{w}_k s_k + \mathbf{h}_k^H \sum_{j \neq k}^K \mathbf{w}_j s_j + n_k, \quad (1)$$

where $\mathbf{h}_k \in \mathbb{C}^{N_t}$ denotes the channel between the BS and user k , and $n_k \sim \mathcal{CN}(0, \sigma_{ck}^2)$ represents additive white Gaussian noise (AWGN) with variance σ_{ck}^2 . We adopt the Rician fading model for $\mathbf{h}_k, \forall k$. The SINR of the intended symbol at user k can be expressed as

$$\gamma_{ck} = \frac{|\mathbf{h}_k^H \mathbf{w}_k|^2}{\sum_{j \neq k}^K |\mathbf{h}_k^H \mathbf{w}_j|^2 + \sigma_{ck}^2}. \quad (2)$$

After transmission, the BS radar antennas receive echos reflected by the M sensed targets as well as C clutter scatterers around them. The received echo signal at the BS is written as

$$\mathbf{y}_s = \sum_{m=1}^M \mathbf{G}_m \mathbf{x} + \sum_{j=M+1}^{M+C} \mathbf{G}_j \mathbf{x} + \mathbf{n}_s, \quad (3)$$

where $\mathbf{G}_i = \zeta_{si} \alpha_{si} \mathbf{a}_r(\varphi_i) \mathbf{a}_t^H(\varphi_i), i = \{1, \dots, M + C\}$, and $\mathbf{n}_s \sim \mathcal{CN}(0, \sigma_s^2 \mathbf{I})$ is AWGN. Here, we consider line-of-sight (LoS) channels between the BS and the target/clutters, which are assumed to be known for beamforming design [15], [16], [28]. In practice, LoS channel estimation can be performed efficiently using algorithms such as MUSIC. Parameters ζ_{si} , α_{si} , and φ_i represent the path loss, complex gain, and angle associated with target/clutter i , while $\mathbf{a}_r(\cdot)$ and $\mathbf{a}_t(\cdot)$ are the normalized receive and transmit array steering vectors. The BS employs a receive combining matrix $\mathbf{F} = [\mathbf{f}_1, \dots, \mathbf{f}_M] \in \mathbb{C}^{N_r \times M}$, such that the received signal associated with target m is given by

$$r_m = \mathbf{f}_m^H \mathbf{y}_s = \mathbf{f}_m^H \mathbf{G}_m \mathbf{x} + \mathbf{f}_m^H \sum_{j \neq m}^{M+C} \mathbf{G}_j \mathbf{x} + \mathbf{f}_m^H \mathbf{n}_s. \quad (4)$$

Thus, the SCNR can be expressed as

$$\gamma_{sm} = \frac{\|\mathbf{f}_m^H \mathbf{G}_m \mathbf{W}\|^2}{\sum_{j \neq m}^{M+C} \|\mathbf{f}_m^H \mathbf{G}_j \mathbf{W}\|^2 + N_r \sigma_s^2 \|\mathbf{f}_m\|^2}. \quad (5)$$

Problem Formulation: We aim to jointly optimize the transmit precoding matrix \mathbf{W} and receive combining matrix \mathbf{F} to 1) ensure *fairness* among communications users and sensed targets; and 2) achieve a balanced tradeoff between communications and sensing performance. To achieve these goals, we employ the utility function $h(\mathbf{W}, \mathbf{F}) = \min_{k \in \mathcal{K}} \{\log(1 + \gamma_{ck})\} + \delta \min_{m \in \mathcal{M}} \{\log(1 + \gamma_{sm})\}$, where $\log(1 + \gamma_{ck})$ and $\log(1 + \gamma_{sm})$ represent the communications rate and sensing MI [22], [35], respectively, and $\delta \geq 0$ balances their performance tradeoff. The joint design problem is then formulated as

$$\max_{\mathbf{W} \in \mathcal{S}, \mathbf{F}} h(\mathbf{W}, \mathbf{F}), \quad (6)$$

where $\mathcal{S} = \{\mathbf{W} : \text{diag}(\mathbf{W}\mathbf{W}^H) \preceq \frac{P_t}{N_t} \mathbf{1}_{N_t}\}$. The max-min objective guarantees fairness while the communications and sensing performance are balanced by adjusting δ . However, problem (6) is challenging, as the utility function includes the non-smooth point-wise minima in $h(\mathbf{W}, \mathbf{F})$, non-convex fractional SINRs and SCNRs, and strongly coupled variables.

III. MODEL-BASED ML OPTIMIZER

We herein propose a learning-aided optimizer for fairness JCAS beamforming. Specifically, we first formulate a surrogate objective to cope with the complex objective in (6). We identify an AO method suitable for the resulting optimization. Then, we leverage model-based ML, and particularly deep unfolding [38], to enhance performance by converting the optimizer into a ML model.

Surrogate Objective: Introducing the variables $\mathbf{z}_c = [z_{c1}, \dots, z_{cK}]^T$ and $\mathbf{z}_s = [z_{s1}, \dots, z_{sM}]^T$, we rewrite (6) as

$$\max_{\mathbf{W} \in \mathcal{S}, \mathbf{F}} \min_{\substack{\mathbf{z}_c \in \mathcal{Z}_c, \\ \mathbf{z}_s \in \mathcal{Z}_s}} \left\{ \sum_{k=1}^K z_{ck} r_{ck} + \delta \sum_{m=1}^M z_{sm} r_{sm} \right\}, \quad (7)$$

where $\mathcal{Z}_c = \{\mathbf{z}_c : \mathbf{z}_c \succeq \mathbf{0}, \mathbf{1}_K^T \mathbf{z}_c = 1\}$ and $\mathcal{Z}_s = \{\mathbf{z}_s : \mathbf{z}_s \succeq \mathbf{0}, \mathbf{1}_M^T \mathbf{z}_s = 1\}$ are compact convex simplices, and $r_{ck} = \log(1 + \gamma_{ck}), r_{sm} = \log(1 + \gamma_{sm})$. As the optimal solution is located at the vertex of the simplices, solving (7) directly can lead to oscillation near the optimal point. To address this, we approximate $\{\mathbf{z}_c, \mathbf{z}_s\}$ by

$$z_{ck} \approx \frac{\exp(-\mu_c r_{ck})}{\sum_{j=1}^K \exp(-\mu_c r_{cj})}, z_{sm} \approx \frac{\exp(-\mu_s r_{sm})}{\sum_{j=1}^M \exp(-\mu_s r_{sj})}, \forall m, k, \quad (8)$$

where μ_s and μ_c are continuous-valued parameters. These approximations become tight as $\mu_s, \mu_c \rightarrow \infty$ [39]. To deal with the non-convex objective, we introduce auxiliary variables $\boldsymbol{\xi}_c = [\xi_{c1}, \dots, \xi_{cK}]^T \in \mathbb{R}^K$, $\boldsymbol{\xi}_s = [\xi_{s1}, \dots, \xi_{sM}]^T \in \mathbb{R}^M$, $\boldsymbol{\theta}_c = [\theta_{c1}, \dots, \theta_{cK}]^T \in \mathbb{C}^K$, and $\boldsymbol{\Theta}_s = [\boldsymbol{\theta}_s^H, \dots, \boldsymbol{\theta}_s^H]^H \in \mathbb{R}^{M \times K}$, and employ the quadratic transformation [40, Theorem 1] to obtain an equivalent but more tractable problem

$$\max_{\substack{\mathbf{W} \in \mathcal{S}, \\ \mathbf{F}, \boldsymbol{\xi}, \boldsymbol{\Theta}}} \min_{\substack{\mathbf{z}_c \in \mathcal{Z}_c, \\ \mathbf{z}_s \in \mathcal{Z}_s}} \left\{ \sum_{k=1}^K z_{ck} O_{ck} + \delta \sum_{m=1}^M z_{sm} O_{sm} \right\}, \quad (9)$$

where $\boldsymbol{\xi} = \{\boldsymbol{\xi}_c, \boldsymbol{\xi}_s\}$, $\boldsymbol{\Theta} = \{\boldsymbol{\theta}_c, \boldsymbol{\Theta}_s\}$,

$$O_{ck} = \log(1 + \xi_{ck}) + 2\sqrt{1 + \xi_{ck}} \Re\{\mathbf{h}_k^H \mathbf{w}_k \boldsymbol{\theta}_{ck}^*\} - \xi_{ck} - |\theta_{ck}|^2 \left(\sum_{j=1}^K |\mathbf{h}_k^H \mathbf{w}_j|^2 + \sigma_{ck}^2 \right), \quad (10)$$

$$O_{sm} = \log(1 + \xi_{sm}) + 2\sqrt{1 + \xi_{sm}} \Re\{\mathbf{f}_m^H \mathbf{G}_m \mathbf{W} \boldsymbol{\theta}_s^H\} - \xi_{sm} - \|\boldsymbol{\theta}_s\|^2 \left(\sum_{j=1}^{M+C} \|\mathbf{f}_m^H \mathbf{G}_j \mathbf{W}\|^2 + N_r \sigma_s^2 \|\mathbf{f}_m\|^2 \right). \quad (11)$$

AO Optimizer: We can solve the problem (9) via AO. Specifically, the auxiliary variables $\{\boldsymbol{\xi}, \boldsymbol{\Theta}\}$ are related to the design variables \mathbf{F} and \mathbf{W} via

$$\xi_{ck} = \gamma_{ck}, \xi_{sm} = \gamma_{sm}, \theta_{ck} = \frac{\sqrt{1 + \xi_{ck}} \mathbf{h}_k^H \mathbf{w}_k}{\sum_{j=1}^K |\mathbf{h}_k^H \mathbf{w}_j|^2 + \sigma_{ck}^2}, \quad (12a)$$

$$\boldsymbol{\theta}_s = \frac{\sqrt{1 + \xi_{sm}} \mathbf{f}_m^H \mathbf{G}_m \mathbf{W}}{\sum_{j=1}^{M+C} \|\mathbf{f}_m^H \mathbf{G}_j \mathbf{W}\|^2 + N_r \sigma_s^2 \|\mathbf{f}_m\|^2}. \quad (12b)$$

Hence, given $\{\boldsymbol{\xi}, \boldsymbol{\Theta}\}$ and \mathbf{W} , \mathbf{F} is updated by

$$\mathbf{f}_m = \frac{\sqrt{1 + \xi_{sm}}}{\|\boldsymbol{\theta}_s\|^2} \left(\sum_{j=1}^{M+C} \mathbf{G}_j \mathbf{W} \mathbf{W}^H \mathbf{G}_j^H + N_r \sigma_s^2 \mathbf{I} \right)^{-1} \mathbf{G}_m \mathbf{W} \boldsymbol{\theta}_s^H. \quad (13)$$

The proposed AO method thus operates in an iterative fashion. In each iteration, AO first uses \mathbf{F} and \mathbf{W} from the previous iteration to set the auxiliary variables (12), which in turn are used to update \mathbf{F} via (13). Then, \mathbf{W} is updated using projected gradient descent (PGD). Specifically, we define $\mathbf{H} = [\mathbf{h}_1, \dots, \mathbf{h}_K]$, $\mathbf{X} = \delta \sum_{m=1}^M z_{sm} \sqrt{1 + \xi_{sm}} \boldsymbol{\theta}_s^H \mathbf{f}_m^H \mathbf{G}_m$, $\mathbf{Y} = \delta \sum_{j=1}^{M+C} \mathbf{G}_j \left(\sum_{m=1}^M z_{sm} \|\boldsymbol{\theta}_s\|^2 \mathbf{f}_m \mathbf{f}_m^H \right) \mathbf{G}_j$, and

$$\boldsymbol{\Sigma}_1 = \text{diag}\{z_{c1} \sqrt{1 + \xi_{c1}} \theta_{c1}, \dots, z_{cK} \sqrt{1 + \xi_{cK}} \theta_{cK}\}, \quad (14)$$

$$\boldsymbol{\Sigma}_2 = \text{diag}\{z_{c1} |\theta_{c1}|^2, \dots, z_{cK} |\theta_{cK}|^2\}. \quad (15)$$

With the other variables fixed, the subproblem with respect to \mathbf{W} is formulated as $\min_{\mathbf{W} \in \mathcal{S}} g(\mathbf{W})$, where $g(\mathbf{W}) = \text{tr}(\mathbf{W} \mathbf{W}^H (\mathbf{Y} + \mathbf{H} \boldsymbol{\Sigma}_2 \mathbf{H}^H)) - 2\Re\{\text{tr}(\mathbf{W} (\mathbf{X} + \boldsymbol{\Sigma}_1^H \mathbf{H}^H))\}$ is convex with respect to \mathbf{W} . Hence, PGD can solve this problem. The

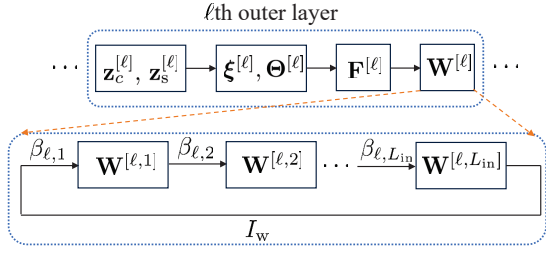


Fig. 1: Proposed model-based DNN structure.

gradient of $g(\mathbf{W})$ is given by

$$\nabla_{\mathbf{W}} g = 2(\mathbf{Y} + \mathbf{H}\Sigma_2\mathbf{H}^H)\mathbf{W} - 2(\mathbf{H}\Sigma_1 + \mathbf{X}^H). \quad (16)$$

Let $\Pi_{\mathcal{S}}(\cdot)$ denote the projection onto the set \mathcal{S} : $\Pi_{\mathcal{S}}(\mathbf{W}) = \sqrt{\frac{P}{N_t}} \text{diag}(\mathbf{W}\mathbf{W}^H)^{-\frac{1}{2}}\mathbf{W}$ where $\text{diag}(\cdot)$ is a diagonal matrix whose diagonal entries are taken from the argument. The PGD update is thus

$$\mathbf{W} \leftarrow \Pi_{\mathcal{S}} \left(\tilde{\mathbf{W}} - \beta \frac{\nabla_{\mathbf{W}} g}{\|\nabla_{\mathbf{W}} g\|_F} \Big|_{\mathbf{W}=\tilde{\mathbf{W}}} \right), \quad (17)$$

where β is the step size and $\tilde{\mathbf{W}}$ is the previous iterate of \mathbf{W} .

Unfolded Optimizer: In the AO procedure, updating \mathbf{W} requires a proper step size to ensure fast convergence. However, selecting an appropriate step size using techniques such as the backtracking search algorithm [41] introduces additional complexity. Furthermore, the parameters $\{\mu_s, \mu_c\}$ also influence performance and typically require manual adjustment based on empirical experience. We overcome these difficulties by converting the AO into a discriminative ML model [42], which can be viewed as a deep neural network (DNN). The DNN is trained to learn iteration-specific step sizes and $\{\mu_s, \mu_c\}$ in an unsupervised manner, based on objective function $h(\mathbf{W}, \mathbf{F})$.

The proposed DNN consists of L_{out} outer layers, and the structure of the ℓ th outer layer is illustrated in Fig. 1. In each outer layer, $\{\mathbf{z}_c, \mathbf{z}_s, \boldsymbol{\xi}, \boldsymbol{\Theta}, \mathbf{F}\}$ and \mathbf{W} are updated successively, where the former ones have closed-form expressions given by (8), (12), and (13). To efficiently obtain \mathbf{W} , we unfold the PGD algorithm into L_{in} inner layers. Specifically, with the trainable step size $\{\beta_{\ell,i}\}_{\ell=1, i=1}^{L_{\text{out}}, L_{\text{in}}}$, $\mathbf{W}^{[\ell,i]}$ is updated by

$$\mathbf{W}^{[\ell,i]} \leftarrow \Pi_{\mathcal{S}} \left(\mathbf{W}^{[\ell,i-1]} - \beta_{\ell,i} \frac{\nabla_{\mathbf{W}} g}{\|\nabla_{\mathbf{W}} g\|_F} \Big|_{\mathbf{W}=\mathbf{W}^{[\ell,i-1]}} \right). \quad (18)$$

In each iteration, \mathbf{F} is obtained directly with closed-form solution (13). In contrast, \mathbf{W} is updated over unfolded DNN layers, and its update speed is restricted by the power constraint. Through simulations, we found that the update speed of \mathbf{W} is much slower than that of \mathbf{F} , causing slow convergence of the overall algorithm. To overcome this, we propose updating \mathbf{W} over I_w iterations of the L_{in} inner layers. Our simulations show that adjusting I_w can significantly accelerate the convergence, as will be demonstrated in Section IV.

The proposed AO-unfolded ML algorithm for solving (6) is outlined in Algorithm 1. The input to the algorithm, denoted by \mathbf{d} , is the system configuration $\mathbf{d} = \{\mathbf{H}, \mathbf{G}, P_t, \sigma_{\text{ck}}, \sigma_s\}$, where \mathbf{G} represents $\{\mathbf{G}_m\}_{m=1}^{M+C}$. In step 1, we first set $\{\mu_s, \mu_c\}$ with predefined values and initialize \mathbf{W} and \mathbf{F} for each channel realization. Steps 2–13 represent the update of $\{\mathbf{z}_c, \mathbf{z}_s, \boldsymbol{\xi}, \boldsymbol{\Theta}, \mathbf{F}, \mathbf{W}\}$ with L_{out} outer layers, while in steps 5–12, the update of \mathbf{W} is performed with L_{in} inner layers and

Algorithm 1: Unfolded AO Optimizer

Input: $\mathbf{d} = \{\mathbf{H}, \mathbf{G}, P_t, \sigma_{\text{ck}}, \sigma_s\}$
Output: \mathbf{F}, \mathbf{W}

- 1 Initialization: Set $\{\mu_s, \mu_c\}$ and generate $\{\mathbf{F}^{[0]}, \mathbf{W}^{[0]}\}$.
- 2 **for** $\ell = 1, \dots, L_{\text{out}}$ **do**
- 3 Update $\mathbf{z}_c^{[\ell]}, \mathbf{z}_s^{[\ell]}$ based on (8) with $\{\mu_s, \mu_c\}$.
- 4 Update $\boldsymbol{\xi}^{[\ell]}, \boldsymbol{\Theta}^{[\ell]}$, and $\mathbf{F}^{[\ell]}$ based on (12) and (13).
- 5 $\mathbf{W}^{[\ell,0]} \leftarrow \mathbf{W}^{[\ell-1]}$.
- 6 **for** $j = 1, \dots, I_w$ **do**
- 7 **for** $i = 1, \dots, L_{\text{in}}$ **do**
- 8 Update $\mathbf{W}^{[\ell,i]}$ by (18).
- 9 **end**
- 10 $\mathbf{W}^{[\ell,0]} \leftarrow \mathbf{W}^{[\ell, L_{\text{in}}]}$
- 11 **end**
- 12 $\mathbf{W}^{[\ell]} \leftarrow \mathbf{W}^{[\ell, L_{\text{in}}]}$.
- 13 **end**
- 14 $\mathbf{F} = \mathbf{F}^{[L_{\text{out}}]}, \mathbf{W} = \mathbf{W}^{[L_{\text{out}}]}$.

I_w loops. We obtain $\{\mathbf{F}, \mathbf{W}\}$ from the output of the L_{out} th outer layer, as in step 14.

The complexity of Algorithm 1 is dominated by the matrix multiplications required to update \mathbf{F} , \mathbf{Y} , and \mathbf{W} . Computing \mathbf{F} and \mathbf{Y} results in a complexity of $\mathcal{O}(L_{\text{out}}(M + C)(N_t^2 N_r + N_t N_r^2))$. The complexity of updating \mathbf{W} is $\mathcal{O}(2L_{\text{out}} L_{\text{in}} I_w K N_t^2)$. Therefore, the overall complexity is approximately $L_{\text{out}} \mathcal{O}((M + C)(N_t^2 N_r + N_t N_r^2) + 2L_{\text{in}} I_w K N_t^2)$.

Training: The trainable parameters of Algorithm 1 are thus $\phi = \{\mu_s, \mu_c, \{\beta_{\ell,i}\}_{\ell=1, i=1}^{L_{\text{out}}, L_{\text{in}}}\}$. These are learned from a data set \mathcal{D} comprised of B potential JCAS settings, i.e., $\mathcal{D} = \{\mathbf{d}_b\}_{b=1}^B$. While the AO optimizer is derived from the proposed surrogate objective, the parameters of the unfolded AO are trained to maximize the original objective in (6).

Specifically, letting $\mathbf{W}^{[\ell]}(\mathbf{d}; \phi)$, $\mathbf{F}^{[\ell]}(\mathbf{d}; \phi)$ denote the output of the ℓ th iteration of Algorithm 1 with input \mathbf{d} and parameters ϕ , the training loss used to guide the tuning of ϕ from \mathcal{D} is

$$\mathcal{L}_{\mathcal{D}}(\phi) = -\frac{1}{B} \sum_{b=1}^B \sum_{\ell=1}^{L_{\text{out}}} \lambda_{\ell} h(\mathbf{W}^{[\ell]}(\mathbf{d}_b; \phi), \mathbf{F}^{[\ell]}(\mathbf{d}_b; \phi)), \quad (19)$$

where $\lambda_{\ell} = \frac{1}{\ell}$ is the weight associated with the ℓ th outer layer. The decreasing weight sequence prioritizes the initial layers for learning, allowing the solution to rapidly approach the optimal point in the beginning, and then gradually refined by the latter layers. In doing so, the overall convergence speed is slightly improved based on our simulations.

IV. NUMERICAL RESULTS

In this section, we evaluate the performance of the proposed model-based ML algorithm¹. Throughout the simulations, we set $N_t = N_r = 16$, $M = C = 2$, and $K = 4$ for training and testing unless otherwise stated. We set Rician factor of 3 dB to generate $\mathbf{h}_k, \forall k$. The path loss is modeled as $\zeta_x = \zeta_0 d_x^{\epsilon_x}$, where $\zeta_0 = -30$ dB is the reference path loss at 1 m, and $(\cdot)_x$ with $x \in \{c, s\}$ represent the parameters for communications and sensing channels, respectively. Accordingly, we assume the path loss exponents $\epsilon_c = 3$, $\epsilon_s = 2$ and distances from the

¹The code source is available online at https://github.com/WillysMa/JCAS_BF_Design_MaxMin.

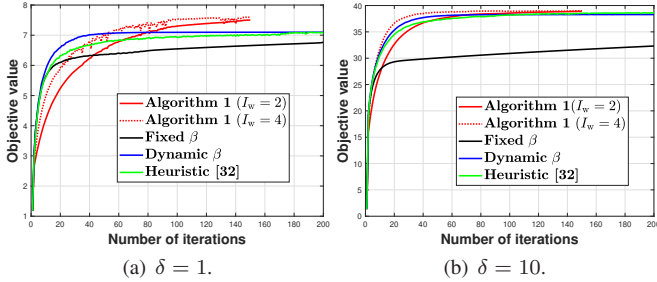


Fig. 2: Convergence of Algorithm 1 with $\delta \in \{1, 10\}$.

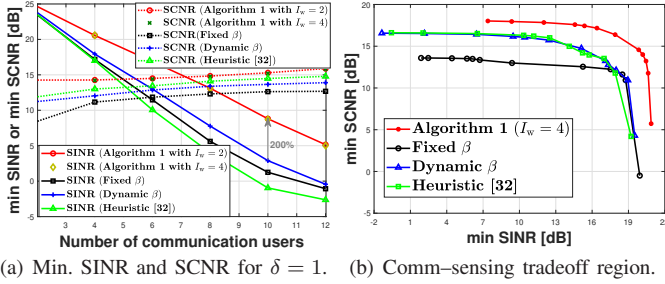


Fig. 3: Minimum SINR and minimum SCNR and their tradeoff.

BS to the k th user and m th target as $d_{c,k} = 100 + 20\eta_{c,k}$ and $d_{s,m} = 10 + 2\eta_{s,m}$, where $\eta_{ck}, \eta_{sm} \sim \mathcal{N}(0, 1)$. The transmit power is set to achieve a signal-to-noise ratio (SNR) of $\frac{P_t}{\sigma_s} = 20$ dB, with $\sigma_s = \sigma_{ck} = -80$ dBm.

The sizes of the training and testing sets are 500 and 100, respectively, using the general Rician fading model for communications channels. We train over over 30 epochs with batch size of 32. For initialization, we set $\beta_{\ell,i} = 0.01, \forall \ell, i$, and initialize \mathbf{W} based on the maximum ratio transmission method, i.e., $\mathbf{W}^{[0]} = \mathbf{\Pi}_S(\mathbf{H})$. Furthermore, we set $\mu_s = \mu_c = 10$ based on empirical simulations, which ensures the convergence of both the proposed method and the compared scheme in [32]. We set $\mathbf{F}^{[0]}$ by maximizing the SCNR in (5) for the M targets, which is a generalized eigenvalue problem whose solution is established in the literature [43]. For all results reported below, we set $L_{\text{out}} = 150, L_{\text{in}} = 3, I_w = 2$ for training. All results are obtained by averaging over 100 channel realizations.

For comparison, we consider AO optimizers employing either fixed (“Fixed β ”) or dynamic (“Dynamic β ”) step sizes to update \mathbf{W} . For the former, the step size is set to 0.01, which is the same as the initial value for $\beta_{\ell,i} \forall \ell, i$. For the latter, the step size for each \mathbf{W} update is found by the backtracking line search method. The steps of the two algorithms are the same as in Algorithm 1 except we set $I_w = 1$. We also compare with the heuristic method for updating \mathbf{W} in [32].

In Figs. 2(a) and 2(b), we show the convergence of the considered schemes with $\delta \in \{1, 10\}$ and $I_w = \{2, 4\}$. It is observed that the proposed algorithm converges to the largest objective values with fewer iterations compared to the benchmark schemes. The gain is more significant for smaller δ . Furthermore, increasing I_w accelerates the convergence and leads to a higher objective value of the proposed method. However, a large I_w may cause oscillation near the local optimal point, as can be observed in Fig. 2(a) for $I_w = 4$.

Fig. 3(a) shows the minimum SINRs and SCNRs for $K = \{2, 4, \dots, 12\}$ and $\delta = 1$. As K increases, inter-user

TABLE I: Average run time (s) of the considered algorithms.

Algorithm	$K = 6$	$K = 8$	$K = 10$	$K = 12$
Fixed β	0.4482	0.9897	1.420	1.736
Heuristic [32]	0.3504	0.4352	0.4740	0.4943
Dynamic β	0.1985	0.2892	0.3540	0.2775
Algorithm 1 ($I_w = 2$)	0.2249	0.2327	0.2308	0.2313
Algorithm 1 ($I_w = 4$)	0.1730	0.1704	0.1774	0.1719

interference becomes more significant. Thus, the minimum SINR of all the schemes considered decreases, contributing less to the objective function $h(\mathbf{W}, \mathbf{F})$ in (6). As a result, the minimum SCNR increases slightly with K . We note here that the proposed unfolding model is trained with the dataset obtained for $K = 4$. However, it generalizes well for various values of K during online inference because its model structure is independent of K . Among the compared schemes, the proposed method achieves the largest minimum SINR/SCNR, with its gain being more significant for the communications functions. With $K = 10$, the SINR improves by up to 200% compared to the scheme using backtracking line search. We further show the tradeoff between the minimum SINR and SCNR of the considered schemes for $\delta \in [0, 100]$ in Fig. 3(b). It is seen that the proposed scheme achieves the best tradeoff between the minimum SINR and minimum SCNR.

In Table I, we show the average run time of the considered algorithms for $\delta = 1$. All the compared schemes are performed on the same platform. Based on the results in Fig. 2(a), we set $L_{\text{out}} = \{150, 100\}$ for $I_w = \{2, 4\}$, respectively, for Algorithm 1. Meanwhile, the benchmark schemes are set to run until convergence. It is observed from Table I that the proposed scheme with $I_w = 4$ performs the fastest, and its run time remains almost constant when K increases. Furthermore, the reduction in run time of the proposed scheme is more significant with larger K . For example, when $K = 10$, Algorithm 1 with $I_w = 4$ achieves a run time reduction of 67%, 75%, and 92% compared to the dynamic step size strategy, the heuristic method, and the fixed step size strategy, respectively. Note that this reduction is achieved while better performance is guaranteed, as seen from Fig. 3(a). The superior performance of Algorithm 1 over the conventional optimization-based approaches is due primarily to the fact that the step sizes are learned from the data, which enhances convergence.

V. CONCLUSIONS

This paper proposed an efficient beamforming design for multi-user multi-target JCAS systems, aiming to ensure fairness and balance between communications and sensing performances. We jointly optimized the transmit and receive beamformers to maximize the weighted sum of the minimum communications rate and sensing MI. To address this challenging problem, we proposed a model-based ML algorithm. Numerical results demonstrate that our algorithm scales well with the number of communications users while delivering better performance with shorter run time compared to conventional optimization-based methods.

REFERENCES

- [1] J. A. Zhang, X. Huang, Y. J. Guo, J. Yuan, and R. W. Heath, "Multibeam for joint communication and radar sensing using steerable analog antenna arrays," *IEEE Trans. Veh. Technol.*, vol. 68, no. 1, pp. 671–685, 2018.
- [2] D. Ma, N. Shlezinger, T. Huang, Y. Liu, and Y. C. Eldar, "Joint radar-communication strategies for autonomous vehicles: Combining two key automotive technologies," *IEEE Signal Process. Mag.*, vol. 37, no. 4, pp. 85–97, 2020.
- [3] J. A. Zhang, F. Liu, C. Masouros, R. W. Heath, Z. Feng, L. Zheng, and A. Petropulu, "An overview of signal processing techniques for joint communication and radar sensing," *IEEE J. Sel. Topics Signal Process.*, vol. 15, no. 6, pp. 1295–1315, 2021.
- [4] A. Liu, Z. Huang, M. Li, Y. Wan, W. Li, T. X. Han, C. Liu, R. Du, D. K. P. Tan, J. Lu, et al., "A survey on fundamental limits of integrated sensing and communication," *IEEE Commun. Surveys Tuts.*, vol. 24, no. 2, pp. 994–1034, 2022.
- [5] U. Demirhan and A. Alkhateeb, "Integrated sensing and communication for 6G: Ten key machine learning roles," *IEEE Commun. Mag.*, vol. 61, no. 5, pp. 113–119, 2023.
- [6] N. T. Nguyen, M. Ma, O. Lavi, N. Shlezinger, Y. C. Eldar, A. L. Swindlehurst, and M. Juntti, "Deep unfolding hybrid beamforming designs for THz massive MIMO systems," *IEEE Trans. Signal Process.*, vol. 71, pp. 3788–3804, 2023.
- [7] M. Ma, N. T. Nguyen, I. Atzeni, and M. Juntti, "Joint beamforming design and bit allocation in massive MIMO with resolution-adaptive ADCs," *arXiv preprint arXiv:2407.03796*, 2024.
- [8] J. Johnston, L. Venturino, E. Grossi, M. Lops, and X. Wang, "MIMO OFDM dual-function radar-communication under error rate and beam-pattern constraints," *IEEE J. Sel. Areas Commun.*, vol. 40, no. 6, pp. 1951–1964, 2022.
- [9] A. Hassaniien, M. G. Amin, Y. D. Zhang, and F. Ahmad, "Dual-function radar-communications: Information embedding using sidelobe control and waveform diversity," *IEEE Trans. Signal Process.*, vol. 64, no. 8, pp. 2168–2181, 2016.
- [10] T. Huang, N. Shlezinger, X. Xu, Y. Liu, and Y. C. Eldar, "MAJoRCom: A dual-function radar communication system using index modulation," *IEEE Trans. Signal Process.*, vol. 68, pp. 3423–3438, 2020.
- [11] F. Liu, C. Masouros, A. Li, H. Sun, and L. Hanzo, "MU-MIMO communications with MIMO radar: From co-existence to joint transmission," *IEEE Trans. Wireless Commun.*, vol. 17, no. 4, pp. 2755–2770, 2018.
- [12] X. Liu, T. Huang, N. Shlezinger, Y. Liu, J. Zhou, and Y. C. Eldar, "Joint transmit beamforming for multiuser MIMO communications and MIMO radar," *IEEE Trans. Signal Process.*, vol. 68, pp. 3929–3944, 2020.
- [13] C. Qi, W. Ci, J. Zhang, and X. You, "Hybrid beamforming for millimeter wave MIMO integrated sensing and communications," *IEEE Commun. Lett.*, vol. 26, no. 5, pp. 1136–1140, 2022.
- [14] W. Chen, Y. Deng, C. Guo, Y. Ma, and B. Liao, "Transmit beamforming optimization for MIMO-ISAC systems with hybrid beamforming," in *Proc. IEEE Int. Conf. Acoust., Speech, Signal Processing*, 2024.
- [15] F. Liu, Y.-F. Liu, A. Li, C. Masouros, and Y. C. Eldar, "Cramér-Rao bound optimization for joint radar-communication beamforming," *IEEE Trans. Signal Process.*, vol. 70, pp. 240–253, 2021.
- [16] X. Song, J. Xu, F. Liu, T. X. Han, and Y. C. Eldar, "Intelligent reflecting surface enabled sensing: Cramér-Rao bound optimization," *IEEE Trans. Signal Process.*, vol. 71, pp. 2011–2026, 2023.
- [17] Q. Zhu, M. Li, R. Liu, and Q. Liu, "Cramér-Rao bound optimization for active RIS-empowered ISAC systems," *arXiv preprint arXiv:2309.09207*, 2023.
- [18] J. Lin, H. Zheng, and X. Feng, "Target parameter estimation with deep unfolding networks for MIMO-OFDM based integrated sensing and communication systems," in *Proc. Int. Conf. on Wireless Commun. and Sign. Proc.*, 2023.
- [19] W. Liu, H. Xu, X. He, Y. Ye, and A. Zhou, "Bi-level deep unfolding based robust beamforming design for IRS-assisted ISAC system," *IEEE Access*, vol. 12, pp. 76663–76672, 2024.
- [20] W. Lin, H. Zheng, X. Feng, and Y. Chen, "Deep unfolding network for target parameter estimation in OTFS-based ISAC systems," in *Proc. IEEE Wireless Commun. and Networking Conf.*, 2024.
- [21] Z. Chen, J. Wang, Z. Tian, M. Wang, Y. Jia, and T. Q. Quek, "Joint rate splitting and beamforming design for RSMA-RIS-assisted ISAC system," *IEEE Wireless Commun. Lett.*, vol. 13, no. 1, pp. 173–177, 2024.
- [22] B. Tang and J. Li, "Spectrally constrained MIMO radar waveform design based on mutual information," *IEEE Trans. Signal Process.*, vol. 67, no. 3, pp. 821–834, 2018.
- [23] N. T. Nguyen, N. Shlezinger, Y. C. Eldar, and M. Juntti, "Multiuser MIMO wideband joint communications and sensing system with sub-carrier allocation," *IEEE Trans. Signal Process.*, vol. 71, pp. 2997–3013, 2023.
- [24] J. Choi, J. Park, N. Lee, and A. Alkhateeb, "Joint and robust beamforming framework for integrated sensing and communication systems," *arXiv preprint arXiv:2402.09155*, 2024.
- [25] X. Liu, T. Huang, and Y. Liu, "Transmit design for joint MIMO radar and multiuser communications with transmit covariance constraint," *IEEE J. Sel. Areas Commun.*, vol. 40, no. 6, pp. 1932–1950, 2022.
- [26] F. Liu, L. Zhou, C. Masouros, A. Li, W. Luo, and A. Petropulu, "Toward dual-functional radar-communication systems: Optimal waveform design," *IEEE Trans. Signal Process.*, vol. 66, no. 16, pp. 4264–4279, 2018.
- [27] Z. Cheng, Z. He, and B. Liao, "Hybrid beamforming design for OFDM dual-function radar-communication system," *IEEE J. Sel. Topics Signal Process.*, vol. 15, no. 6, pp. 1455–1467, 2021.
- [28] N. T. Nguyen, L. V. Nguyen, N. Shlezinger, Y. C. Eldar, A. L. Swindlehurst, and M. Juntti, "Joint communications and sensing hybrid beamforming design via deep unfolding," *IEEE J. Sel. Topics Signal Process.*, 2024.
- [29] P. Wang, J. Fang, X. Zeng, Z. Chen, and H. Li, "Joint transceiver optimization for MmWave/THz MU-MIMO ISAC systems," *arXiv preprint arXiv:2401.17681*, 2024.
- [30] L. Chen, F. Liu, W. Wang, and C. Masouros, "Joint radar-communication transmission: A generalized Pareto optimization framework," *IEEE Trans. Signal Process.*, vol. 69, pp. 2752–2765, 2021.
- [31] Y. Wang, Z. Yang, J. Cui, P. Xu, G. Chen, T. Q. S. Quek, and R. Tafazolli, "Optimizing the fairness of STAR-RIS and NOMA assisted integrated sensing and communication systems," *IEEE Trans. Wireless Commun.*, vol. 23, no. 6, pp. 5895–5907, 2024.
- [32] T. Fang, N. T. Nguyen, and M. Juntti, "Beamforming design for max-min fairness balancing in ISAC systems," in *Proc. IEEE Works. on Sign. Proc. Adv. in Wirel. Comms.*, 2024.
- [33] J. Zhang, M. Liu, J. Tang, N. Zhao, D. Niyato, and X. Wang, "Joint design for RIS-aided ISAC via deep unfolding learning," *IEEE Trans. on Cogn. Commun. Netw.*, Early Access, 2024.
- [34] A. M. Elbir, K. V. Mishra, and S. Chatzinotas, "Terahertz-band joint ultra-massive MIMO radar-communications: Model-based and model-free hybrid beamforming," *IEEE J. Sel. Topics Signal Process.*, vol. 15, no. 6, pp. 1468–1483, 2021.
- [35] Y. Peng, S. Yang, W. Lyu, Y. Li, H. He, Z. Zhang, and C. Assi, "Mutual information-based integrated sensing and communications: A WMMSE framework," *IEEE Wireless Commun. Lett.*, Early Access, 2024.
- [36] N. Shlezinger and Y. C. Eldar, "Model-based deep learning," *Foundations and Trends® in Signal Processing*, vol. 17, no. 4, pp. 291–416, 2023.
- [37] N. Shlezinger, M. Ma, O. Lavi, N. T. Nguyen, Y. C. Eldar, and M. Juntti, "Artificial intelligence-empowered hybrid multiple-input/multiple-output beamforming: Learning to optimize for high-throughput scalable MIMO," *IEEE Veh. Technol. Mag.*, Early Access, 2024.
- [38] N. Shlezinger, Y. C. Eldar, and S. P. Boyd, "Model-based deep learning: On the intersection of deep learning and optimization," *IEEE Access*, vol. 10, pp. 115384–115398, 2022.
- [39] S. Xu, "Smoothing method for minimax problems," *Computational Optimization and Applications*, vol. 20, no. 3, pp. 267–279, 2001.
- [40] K. Shen and W. Yu, "Fractional programming for communication systems—Part I: Power control and beamforming," *IEEE Trans. Signal Process.*, vol. 66, no. 10, pp. 2616–2630, 2018.
- [41] M. Ma, N. T. Nguyen, I. Atzeni, and M. Juntti, "Hybrid receiver design for massive MIMO-OFDM with low-resolution ADCs and oversampling," *arXiv preprint arXiv:2407.04408*, 2024.
- [42] N. Shlezinger and T. Rountenberg, "Discriminative and generative learning for linear estimation of random signals [lecture notes]," *IEEE Signal Process. Mag.*, vol. 40, no. 6, pp. 75–82, 2023.
- [43] B. Ghojogh, F. Karray, and M. Crowley, "Eigenvalue and generalized eigenvalue problems: Tutorial," *arXiv preprint arXiv:1903.11240*, 2019.